

CoA Note No.66



ST. NO. R16,195/A
U.D.C.
AUTH.

THE COLLEGE OF AERONAUTICS  
CRANFIELD



A TRANSISTORIZED RADIATION MONITOR

by

D. C. BROWN and B. P. FARADAY

R 16,195/A



## A TRANSISTORIZED RADIATION MONITOR †

D. C. BROWN, and B. P. FARADAY

*The College of Aeronautics Department of Aircraft Electrical Engineering*

Received 13 December 1956



This paper describes the investigation of a number of possible semiconductor devices which can be used for the detection of radioactive particles. The sensitivities of two types of transistor (a p-n-p alloy junction and an n-p-n grown junction) and a p-n alloy junction diode operated up to its "avalanche" condition were determined. The possible uses of such detectors are discussed and they are shown to be particularly suitable where high rates of counting, with

good efficiency and small detecting area (or low geometry) are required.

A completely transistorized radiation monitor has been developed using a p-n-p transistor as the detector head. This is specifically designed for  $\alpha$ -particle detection but the detector head with slight modification should be suitable for proton or neutron detection.

### 1. Introduction

Crystal particle counters have been described in great profusion in the literature<sup>1,2,3</sup>). Early attempts at detecting particles by means of a crystal detector utilised the effect of electron-hole pair production within a crystal lattice, (often a diamond), by subjecting the crystal to bombardment from some radioactive source. The quantum yield of electron hole pairs is low and a large electric field is required to obtain a sharp current pulse from the system. The same order of field can be produced across a p-n junction and thus a p-n junction can be used as a radioactive particle detector<sup>4,5</sup>).

### 2. The Types of Detector

By using a transistor in the grounded emitter configuration as the detector (in the same fashion as a phototransistor<sup>6</sup>)) the current gain can be utilised to give a greatly increased signal. Current multiplication can also be obtained in the case of a simple p-n junction by using a controlled avalanche effect.

The specific ionisation of the incident radiation determines the magnitude of the current pulse resulting from the arrival of one particle in the sensitive region of the detector. Thus a large

signal should result from  $\alpha$ -particles, smaller ones from neutrons and protons and very small ones from  $\beta$  and  $\gamma$ -rays. The detectors are all light sensitive but if the light falling on them is steady, such as diffuse daylight, this merely results in the d.c. operating point of the detectors changing and a slight increase in the noise level. Fig. 1 shows the arrangement for obtaining a signal from an n-p-n transistor, a p-n-p transistor and a p-n junction diode which exhibited a controlled avalanche effect. In each case the region within a diffusion length of the p-n barrier is sensitive and for the p-n-p alloy junction transistor either the collector or the emitter side can be bombarded. In the case of the junction diode it is obviously better to bombard from the side opposite to the indium dot as a much greater sensitive area is exposed. Fig. 2 shows a photograph taken of the pulses produced by bombarding an n-p-n grown

<sup>1</sup>) R. Hofstadter, Crystal counters, Part. 1, *Nucleonics* (April 1949) 2.

<sup>2</sup>) R. Hofstadter, Crystal counters, Part. 2, *Nucleonics* (May 1949) 29.

<sup>3</sup>) H. Ess and J. Rossel, Some properties of diamond as a crystal counter, *Helv. Phys. Acta* (September 1950) 484.

<sup>4</sup>) K. G. MacKay, A germanium counter, *Phys. Rev.* (November 1949) 1537.

<sup>5</sup>) C. Orman *et al.*, Germanium p-n barriers as counters, *Phys. Rev.* (June 1950) 646.

<sup>6</sup>) J. N. Shive, The properties of germanium phototransistors, *J. Opt. Soc. America* (April 1953) 239.

† This is part of the work submitted by B. P. Faraday for the Diploma of the College of Aeronautics in the Department of Aircraft Electrical Engineering.

junction transistor with 5 MeV  $\alpha$ -particles from a polonium 210 source. The pulses produced are of the order of  $10\mu$  seconds wide, most of the pulse broadening being due to the shunt capacitance of the transistor itself (about  $40\mu\mu\text{F}$ ). The recovery time of the detector is such that pulses separated by  $20\mu$  seconds are clearly resolved.

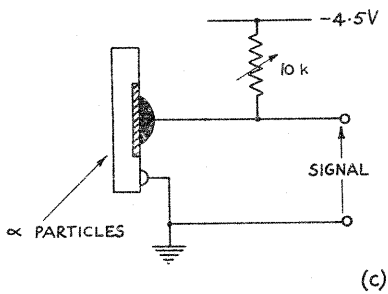
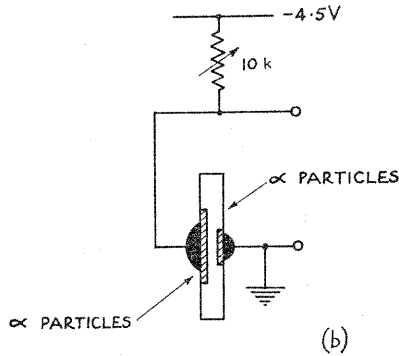
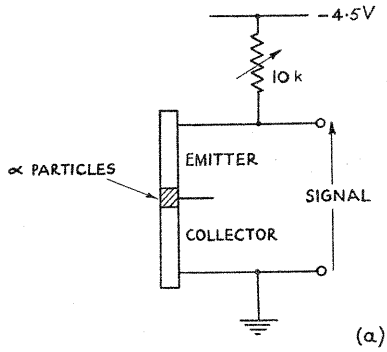


Fig. 1. The method of using (a) an n-p-n junction transistor and (b) a p-n-p alloy junction transistor and (c) a p-n alloy junction diode as detectors of  $\alpha$ -particles.

If the collector current of the detector is increased the sensitivity increases rapidly at first and then becomes almost constant in much the same way as a phototransistor. The graphs

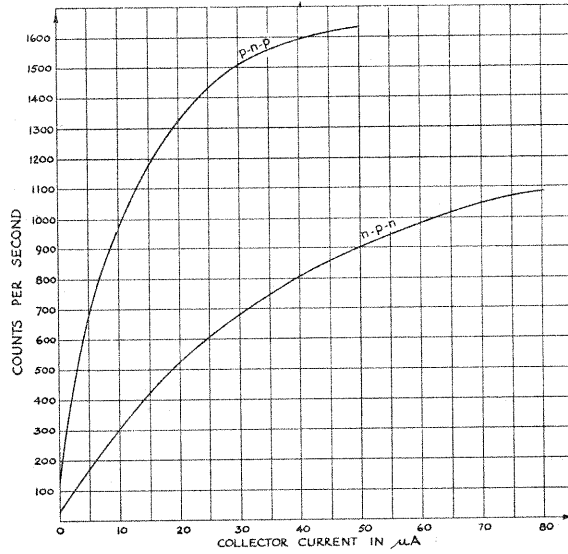


Fig. 3. The variation of counting rate of a p-n-p alloy junction transistor and an n-p-n grown junction transistor as the collector current is varied.

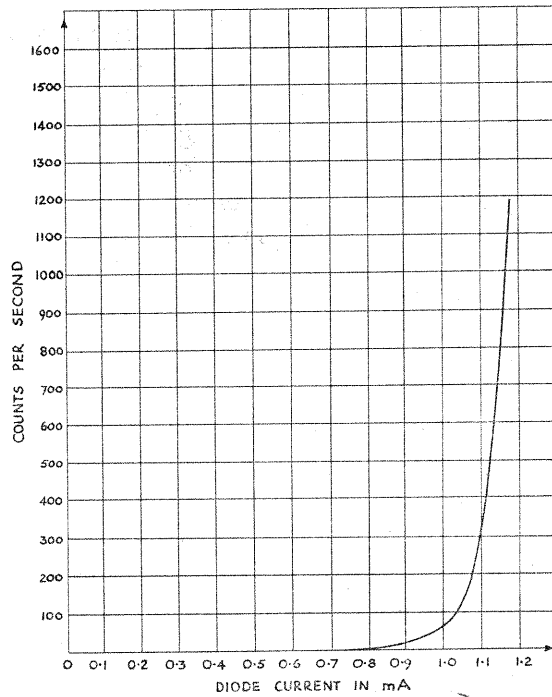


Fig. 4. The variation of counting rate of a p-n junction diode (which exhibited an avalanche effect) with increase in the reverse current.

shown in fig. 3 illustrate this effect by recording the number of pulses which occur when an  $\alpha$ -source is placed a fixed distance from the

detector and the bias current is varied, the clipping level being set so that there was negligible contribution to the count by noise pulses. For the avalanche diode when the reverse current is increased the sensitivity increases very rapidly until a critical stage is reached when an uncontrolled avalanche occurs. The sensitivity curve for an avalanche diode is shown in fig. 4. The p-n-p transistor seems superior to the n-p-n transistor because although its current gain is inherently less than that of the n-p-n transistor the optimum working point is reached at a very much lower bias current. This means that for the same bias voltage supply the signal developed across the resistor in the collector is greater for the p-n-p transistor than for the n-p-n transistor. The avalanche diode is rather an unreliable detector as a small change in bias current results in a large change in sensitivity and if the initial bias condition is near the critical current it is possible for the device to become unstable. If the sensitive area of the detectors is measured experimentally then their

efficiency can be determined by placing them at a known distance from a sub-standard  $\alpha$ -source in a collimating chamber which can be evacuated<sup>7</sup>). Efficiencies, (that is the ratio number of counts recorded to the theoretical number of counts which should occur knowing the d.p.m. of the source and the geometry of the system) up to 0.5 were recorded, depending on the state of the surface contamination.

### 3. The Possible Uses of Semiconductor Radiation Detectors

Such a detector can be of great use where a low geometry counter is required of good efficiency at high rates of counting. Thus it could be used in a probe head for accurately locating metallic plutonium in one of the plutonium alloys. It should also be possible for high energy protons to be detected directly and thus the detector could be used to determine accurately the profile of proton and other beams

<sup>7</sup>) R. Hurst and G. R. Hill, A low geometry proportional counter for  $\alpha$  counting, A.E.R.E. C/R 647.

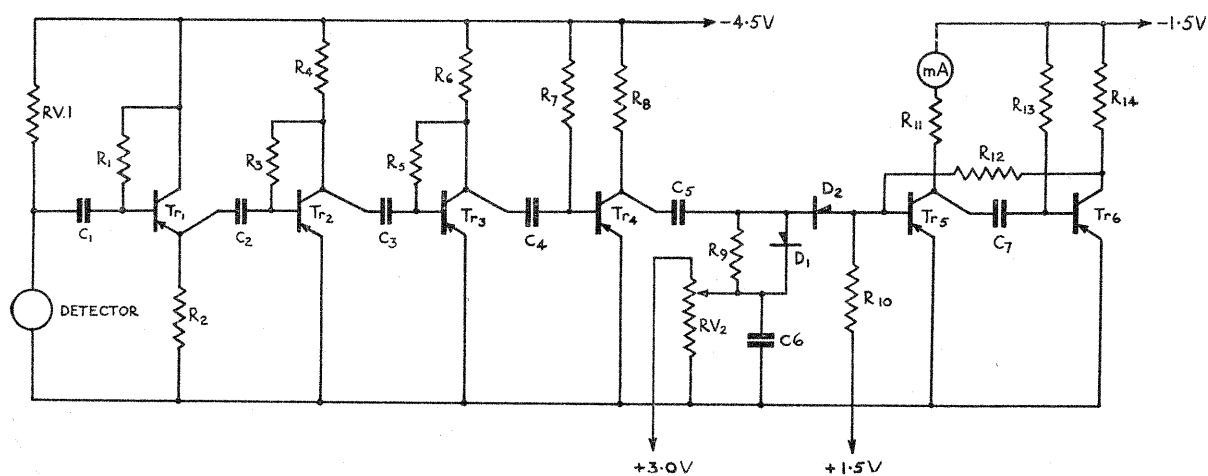


Fig. 5. The circuit diagram of the detector.

$RV_1 = RV_2 = 10k\Omega$	$C_1 = C_2 = C_3 = C_4 = C_6 = 0.04\mu F$
$R_1 = R_3 = R_5 = R_{10} = 220k\Omega$	$C_5 = 0.001\mu F$
$R_2 = R_4 = R_6 = R_8 = 5.6k\Omega$	$C_7 = 0.07$ or $0.007\mu F$
$R_7 = 270k\Omega$	
$R_9 = 100k\Omega$	$D_1 = D_2 = G.E. 10$
$R_{14} = R_{11} = 2.2k\Omega$	$Tr_1 = Tr_2 = Tr_3 = Tr_4 = S.T.C. Type TS 3$
$R_{12} = 10k\Omega$	$Tr_5 = Tr_6 = S.T.C. Type TS 2$
$R_{13} = 22k\Omega$	

from accelerators. It could also be used for detecting thermal neutrons by placing a boron screen between the detector and the source†, or fast neutrons by using a paraffin moderator before the boron screen.

#### 4. The Radiation Monitor

An instrument has been designed incorporating a transistor detector which is primarily intended for  $\alpha$ -particle detection but which, with minor adjustments, could be used for other types of radiation. The instrument is intended to be a portable monitor and is completely transistorized, the circuit diagram being shown in fig. 5.

A high input impedance is required from the detector to the amplifier and if it is to be used on a probe some distance from the amplifier a low output impedance is desirable. A grounded collector transistor or a grounded emitter transistor with degeneration introduced by having an uncoupled emitter resistor will produce the necessary high impedance, the output impedance from a grounded collector stage however is much lower than that from a grounded emitter stage.

Using the  $h$  parameters the input impedance of the grounded collector stage is given by

$$Z_{in}'' = \frac{1 + h_{11}y_L}{h_{22} + y_L(1 + h_{21})} \quad (1)$$

( $y_L$  being the collector load conductance) and of the grounded emitter stage with an emitter resistor  $R_E$  by

$$Z_{in}' = \frac{(h_{11} + R_E)(h_{22} + y_L) - h_{12}h_{21}}{h_{22} + y_L(1 + h_{21})} \quad (2)$$

This must be large with respect to the output impedance of the detector which is approximately equal to  $RV_1$  and should be at least  $50k\Omega$ . Using a transistor with a value of  $h_{21}$  approaching  $-1$  this can be easily attained for both configurations. Assuming values of  $h$  parameters as follows

$$\begin{aligned} h_{22} & 1.0 \mu\text{mho} \\ h_{21} & -0.98 \\ h_{11} & 40 \text{ ohms} \\ h_{12} & 4 \times 10^{-4} \end{aligned}$$

$Z_{in}' = 50k\Omega$  results from  $y_L = 10^{-3}$  mho and  $R_E = 1k\Omega$

The output impedance of a grounded collector stage is given by

$$Z_0'' = \frac{h_{11} + Z_g(1 + h_{21})}{1 + Z_g h_{22}} \quad (3)$$

and for a grounded emitter stage with an emitter resistor  $R_E$

$$Z_0' = \frac{(h_{11} + R_E) + Z_g(1 + h_{21})}{(h_{11} + R_E)h_{22} - h_{21}h_{12} + h_{22}Z_g} \quad (4)$$

If the generator impedance  $Z_g$  is taken to be equal to  $RV_1$ ,  $10k\Omega$  say, and  $R_E$  taken as  $1k\Omega$  for the grounded emitter configuration and the  $h$ -parameters as before then

$$Z_0'' = 240\Omega$$

$$Z_0' = 120k\Omega$$

It is preferable to use a grounded collector stage configuration for the input stage from the detector and the theoretical input and output impedances for the actual circuit shown are

$$Z_{in}'' = 150k\Omega$$

$$Z_0'' = 240\Omega$$

taking into consideration the increase of  $y_L$  because of the presence of the main amplifier.

Transistors  $Tr_2$ ,  $Tr_3$  and  $Tr_4$  constitute a conventional amplifier having a bandwidth of about 50 kc/s. The output from this amplifier is in the form of negative pulses superimposed on a background of noise. In order that the gain of the amplifier can be usefully employed at high counting rates the signal is clamped to a variable positive level by means of the germanium diode  $D_1$  and the signal injected into the monostable multivibrator  $Tr_5$  and  $Tr_6$  by means of another germanium diode  $D_2$  so that only signals more negative than the base potential of  $Tr_5$  can be applied to the multivibrator. The base of  $Tr_5$  is arranged to be at earth potential in its stable state, so that by varying the potentiometer  $RV_2$  the signal can be clipped at any level from zero to three volts.

The multivibrator is a conventional one<sup>8)</sup> with  $Tr_6$  conducting in the stable state. Capacitor

†  $5B^{10} + 0n^1 \rightarrow 3Li^7 + 2He^4$  the  $\alpha$ -particles having an energy of 2.78 MeV.

<sup>8)</sup> J. E. Flood, Junction transistor trigger circuits, Wireless Eng. (May 1955) 122.

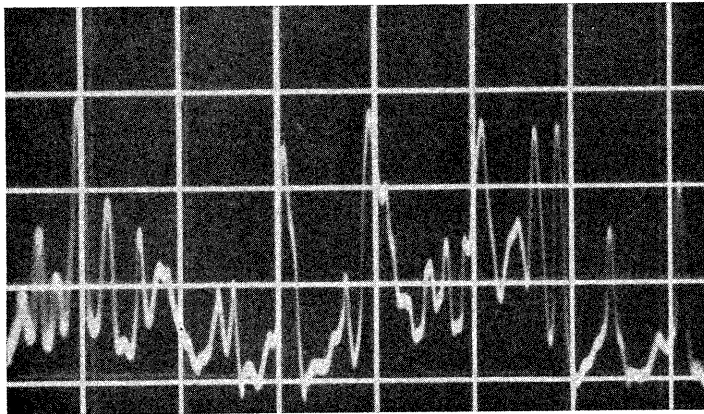


Fig. 2. The output from an n-p-n grown junction transistor when the collector is bombarded with 5 MeV  $\alpha$ -particles. The time scale is such that one square represents  $100\mu$  seconds.

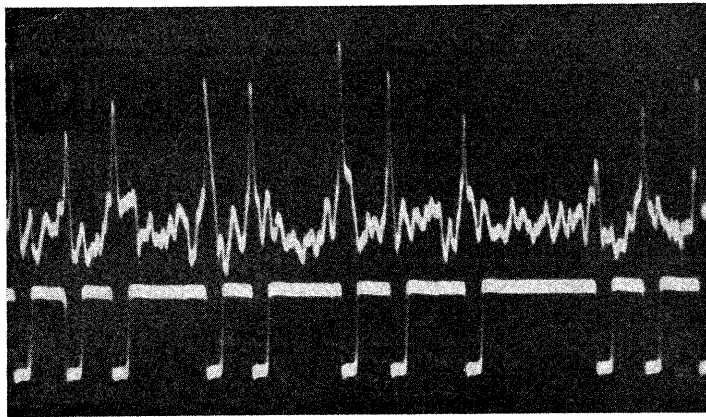


Fig. 7. The output of the amplifier when the detector is bombarded with 5 MeV  $\alpha$ -particles together with the output of the monostable multivibrator.

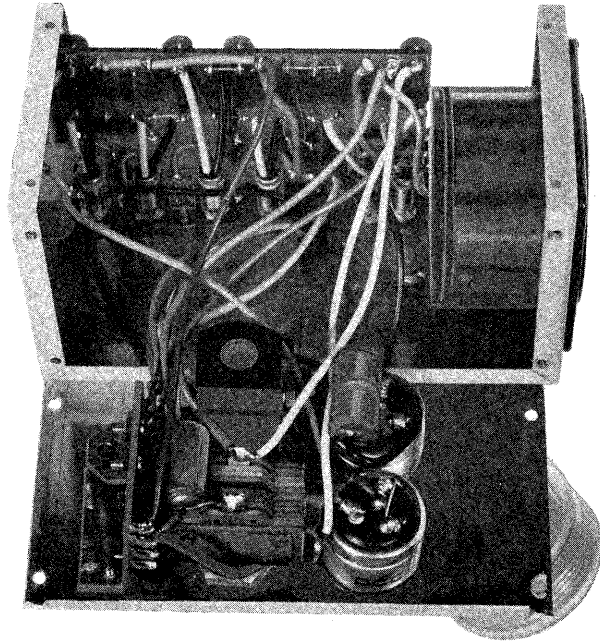


Fig. 8. The monitor showing the indicator meter, control panel and detector with the cover removed.

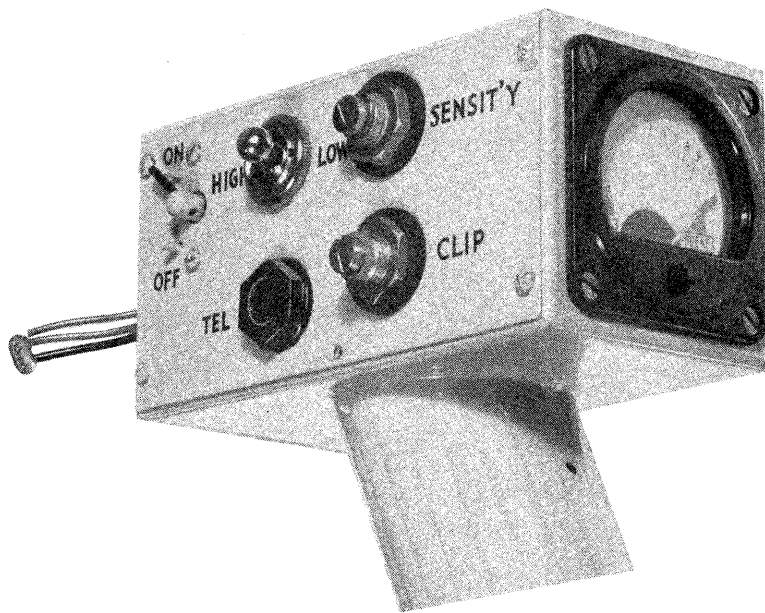


Fig. 9. A view of the interior of the monitor showing constructional details.

$C_7$  can be switched from  $0.007 \mu\text{F}$  to  $0.07 \mu\text{F}$  giving a change in pulse width of almost ten to one. By placing a  $250 \mu\text{A}$  meter in the collector lead of  $\text{Tr}_5$ , the current flowing at any time through the meter is directly proportional to the number of times the multivibrator is triggered and the width of the pulse produced by the multivibrator. This system behaved in a very efficient manner as an integrator, fig. 6 showing how the meter current varies when the frequency of the incoming pulses is varied at both high and low rates of counting. The linearity is not as good as this for random pulses at a high rate, because too many pulses occur during the recovery time of the multivibrator, or at a very low rate, because of the finite inertia of the meter movement. Fig. 7 shows a typical set of random pulses applied to the multivibrator and the resultant multivibrator output.

The complete monitor is shown in fig. 8 and in fig. 9 the side panel is removed to show some of the constructional details. The instrument is completely self-contained, including the battery supplies which are in the handle. When the detector is used for  $\alpha$ -particle detection it can be protected from surface contamination by means of a very thin coating of silicone grease which only reduces the efficiency slightly.

The authors are grateful to the staff of the Department of Aircraft Electrical Engineering, the College of Aeronautics, for their co-operation and the interest shown during the development of this instrument. In particular they would like to thank Mr. E. C. Sills, the head of the Instrumentation Section, who not only built the portable monitor shown in fig. 8, but contributed a considerable amount to the design of the integrator circuit.

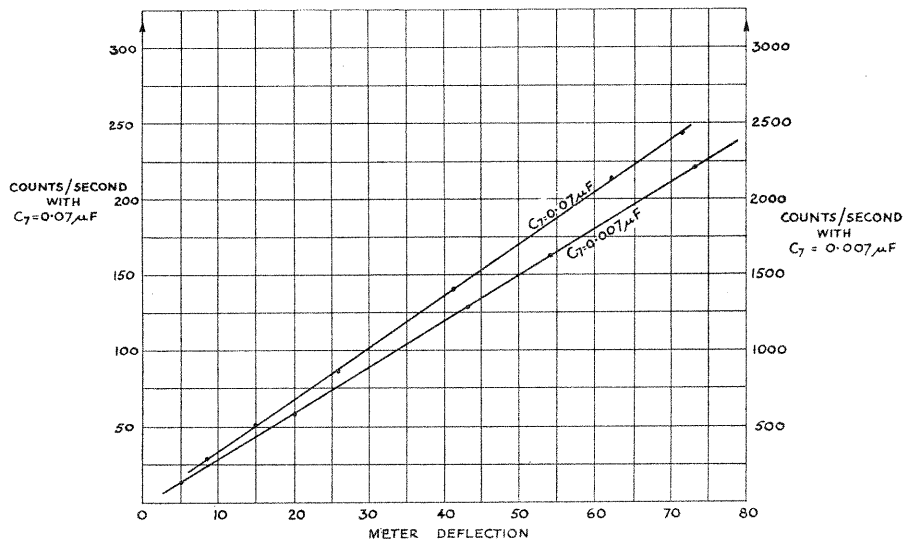


Fig. 6. The calibration of the integrator for two different ranges.